

Abstract

In the selective withdrawal experiment fluid is withdrawn through a tube with its tip suspended a distance S above an unperturbed two-fluid interface. At low withdrawal rates, Q , the interface forms a steady state hump and only the upper fluid is withdrawn. When Q is increased (or S decreased), the interface undergoes a transition so that the lower fluid is entrained with the upper one, forming a thin steady-state spout. Near this discontinuous transition the hump curvature becomes very large and displays power-law scaling behavior. This scaling is used to show that steady-state profiles for humps at different flow rates and tube heights can all be scaled onto a single similarity profile.

Scaling at the selective withdrawal transition

Itai Cohen, Sidney R. Nagel

November 14, 2018

Is it possible to classify topological transitions in nonlinear fluid systems [1, 2, 3, 4] in the same manner as one classifies thermodynamic transitions? When the topological transition involves formation of a singularity in the fluid flows or interface shapes, a similarity solution can provide a simplified description of the flows and help make such a classification [5]. A crucial component to this approach involves determining how characteristic physical quantities and lengths describing the fluid system scale near the singularity. In many cases these singularities manifest themselves in the transition dynamics [6, 7, 8, 9] and do not appear in the steady state flows. Here, we report on steady-state interface profiles near the topological transition associated with the selective withdrawal experiment. Despite the transition being discontinuous, scaling of the interface is observed as the transition is approached.

In the selective withdrawal experiment a tube is immersed in a filled container so that its tip is suspended a height S above an unperturbed interface separating two immiscible fluids. When fluid is pumped out through the tube at low flow rates, Q , only the upper fluid is withdrawn and the interface is deformed into an axi-symmetric steady-state hump (Fig. 1) due to the flows in the upper fluid. The hump grows in height and curvature as Q increases or S decreases until the flows undergo a transition where the lower fluid becomes entrained in a thin axi-symmetric spout along with the upper fluid. The two-fluid interface becomes unbounded in the vertical direction thus changing the topology of the steady state. Once the spout has formed, an increase in Q or decrease in S thickens the spout.

The interfacial profiles at different flow rates and tube heights are recorded. Near the transition, the steady-state radius of curvature of the hump tip is orders of magnitude smaller than the length scales characterizing the boundary conditions (e.g. the tube diameter, D). This separation of length scales suggests that a similarity analysis of the steady-state hump profiles might be possible. However, for the range of parameters explored thus far, even when the system is arbitrarily close to the transition from hump to spout, the mean curvature of the hump tip, κ , while large, remains finite. Nevertheless, by fixing S and looking at the steady-state profiles as Q is increased, we observe that both the hump curvature and height display scaling behavior characteristic of systems approaching a singularity. Since the divergence is cut off before a singularity is reached this transition appears to be “weakly-first-order.”

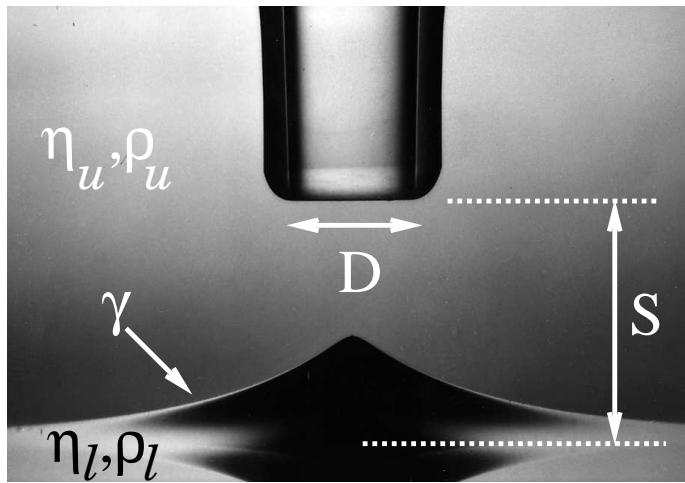


Figure 1: Photograph of two-fluid interface forming a hump. The parameters for this problem include the height of the tube from the unperturbed interface, S , withdrawal rate, Q , surface tension of the two-fluid interface, γ , fluid densities, ρ_u and ρ_l , fluid viscosities, η_u and η_l , tube diameter, D , fluid height above the interface, fluid height below the interface, container size, and surfactant concentration. Here we restrict the investigation to the S vs. Q parameter space and defer discussion of the remaining parameters to [10].

As shown in Fig. 1, the parameters important for this experiment are the upper and lower fluid viscosities and densities ($\eta_u, \eta_l, \rho_u, \rho_l$), interfacial tension (γ), orifice diameter (D), tube height (S), and flow rate (Q). In looking for scaling of the steady-state profiles, care must be taken to design an experimental apparatus capable of isolating the profiles near the transition. Experiments were performed in large tanks (30cm \times 30cm \times 30cm) capable of holding fluid layers that were each about 12 cm in height. To ensure that the upper fluid level remained constant, the withdrawn fluid was recycled back into the container (the bottom fluid layer thickness remains constant when the system is in the hump state). Steady withdrawal rates were achieved by using a gear pump. We verified that for the tube diameter ($D = 0.16$ cm), tube heights (0.1 cm $\leq S \leq 1.1$ cm), and flow rates ($Q \leq 10$ ml/sec) used in the experiments, the container walls were sufficiently distant and the fluid layers sufficiently thick so as not to affect the flows [10]. We measured the upper(Heavy Mineral Oil) and lower(Glycerin-Water mixture) fluid viscosities to be $\eta_u = 2.29$ St and $\eta_l = 1.90$ St, the upper and lower fluid densities to be $\rho_u = 0.88$ g/ml and $\rho_l = 1.24$ g/ml, and the surface tension[11, 12] to be $\gamma = 31$ dynes/cm. Attempts to increase κ near the transition by decreasing γ cause fluid mixing and result in a diffuse interface at high shear rates so that some fraction of the lower fluid is always being withdrawn [13].

While many of the parameters mentioned influence the flows, our understanding of the scaling behavior can be conveyed by focusing on S and Q . We can fix Q and track the development of the hump profiles as a function of S . Below the tube height, S_u , the hump is unstable and undergoes a transition to a spout. Figure 2 shows that $S_u \propto Q^{0.30 \pm 0.05}$ [14]. At low Q the transition is hysteretic: the value of S where the spout becomes unstable and decays back into the hump is larger than S_u . We define the difference of the two heights or hysteresis as ΔS . Figure 2 indicates that the data is consistent with an exponential decrease: $\Delta S = 0.04 \exp^{-Q/0.032}$. For $Q > 0.1$ ml/sec, ΔS was too small to measure.

In order to measure the mean curvature of the hump tip, κ , we first fit the tip of the recorded profile with a Gaussian and then calculate the curvature of the fitting function at the hump tip. Figure 2 also shows the hump height, h_u , and mean radius of curvature, $1/\kappa_u$, at the transition as a function of Q . The dramatic decrease in ΔS coincides with the onset of a flat asymptotic dependence for $1/\kappa_u$ at $Q > 0.1$ ml/sec. We quantify this correlation, by fitting the curvature data with the form $1/\kappa_u = 0.02 + 0.32 \exp^{-Q/0.032}$ which has the same exponential decay with Q as does ΔS . For $Q > 0.1$, ml/sec we find both κ_u , and h_u to be independent of the orifice diameter D [10]. We restrict our scaling analysis to this regime.[15]

Figure 3a plots κ (where $0 \leq \kappa \leq \kappa_u$), versus Q for six data sets corresponding to different values of S . As shown in the inset of Fig. 3a, all fifteen data sets display a power-law divergence for κ , as Q approaches Q_c (a fitting parameter). While the power-law exponents remain constant as S is varied, the prefactors to the power laws, $c_\kappa(S)$, vary slightly with S and are scaled out in the inset. Figure 3b plots the hump height, h_{max} , versus Q . The inset to Fig. 3b shows

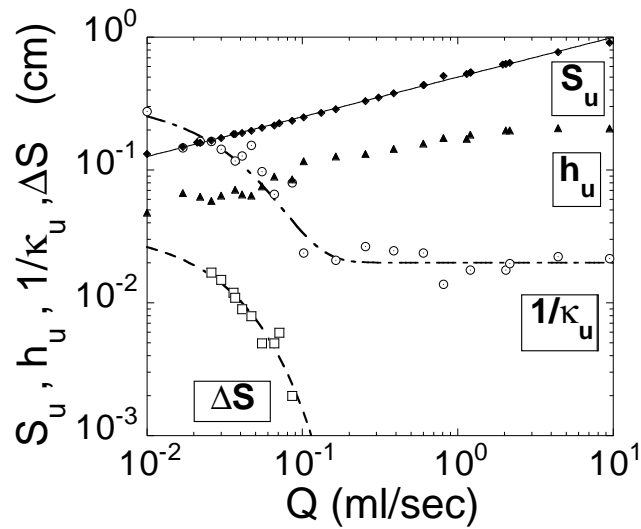


Figure 2: Plots of the transition tube height, S_u , hysteresis, ΔS , hump height, h_u , and mean radius of curvature $1/\kappa_u$, as a function of Q . We find that $S_u \propto Q^{0.30 \pm 0.05}$ (solid line). The ΔS data is fit with an exponential decay (dashed) of the form: $\Delta S = 0.04 \exp^{-Q/0.032}$ although the range is not sufficient to exclude a power-law decay. We fit $1/\kappa_u$ (dash dot), with the form: $1/\kappa_u = 0.02 + 0.32 \exp^{-Q/0.032}$.

that as Q approaches Q_c (obtained from Fig. 3a inset), the hump height approaches h_c (a fitting parameter) as a power law. Once again, the power-law exponents for these data sets are the same over this range of S . The prefactors, $c_h(S)$, are scaled out in the inset. Note that Q_c changes with S indicating that the system can approach a continuous line of divergences. Combining the two scaling dependencies in Fig. 3c, we plot $(h_c - h_{max})/h_{max}$ versus the normalized curvature, κ/n . We find that $(h_c - h_{max})/h_{max}$ scales as $(\kappa/n)^{0.85 \pm 0.09}$ indicating that even though both h_c and the power-law prefactor, n , change with S , the power-law exponents are independent of S for this range of tube heights. Note that $n(S) = c_h(S)[c_\kappa(S)^{0.85}]$. The transition cuts off the evolution of the hump states making it impossible for the system to approach arbitrarily close to the singularity and limiting the precision with which we can determine the exponents.

The scaling observed for h_{max} and κ suggests that the hump profiles should display universal behavior as h_{max} nears h_c . The quantities $1/(\kappa/n)$ and $(h_c - h_{max})/h_{max}$ track how quickly the radial and axial length scales decrease as the system approaches the singularity and are therefore used to scale the profiles. We define the scaled variables:

$$H(R) = \frac{h_c - h(r)}{h_c - h_{max}} \quad \text{and} \quad R = \frac{r\kappa}{n}, \quad (1)$$

where $h(r)$ is the hump profile and h_c is taken from Fig. 3. The transformation shifts the profiles so that under scaling the singularity occurs at the origin and the maximum hump heights occurs at $H = 1$ and $R = 0$. Figure 4 shows eight scaled profiles for the $S = 0.830$ cm data set. In the bottom inset we overlay the hump profiles scaled in the main figure. We find excellent collapse of the profiles. The solid line in Fig. 4 is a power law that fits the data in the region beyond the parabolic tip. The picture that emerges is of a parabolic tip region which decreases in its radial scale and is simultaneously pulled towards the singularity in the axial direction leaving behind it a power-law profile with an exponent of 0.72 ± 0.08 . This exponent is within error (although slightly smaller) of the exponent observed in the scaling relation of Fig. 3c which predicts an exponent of 0.85 ± 0.09 .

Typically, the observed scaling dependencies in these types of problems result from the local stress balance. A scaling analysis where the viscous stresses of the upper and lower fluids balance the stress arising from the interfacial curvature predicts linear scaling dependencies and conical profile shapes. The non-linearity of the observed dependencies indicates that either a different stress balance governs the flows (e.g. only viscous stress due to upper fluid balances stress due to the interface curvature) or that non-local effects are coupling into the solution. A more detailed discussion can be found in [10].

Finally, we compare the similarity curves for five different tube heights in the upper right inset of Fig. 4. The profiles all display the same power-law dependence. Within error, the normalized curvature κ/n (taken from Fig. 3c) can be used to scale the radial components of these profiles and obtain good collapse. In Fig. 3c we find that the normalization prefactors, n , decrease as

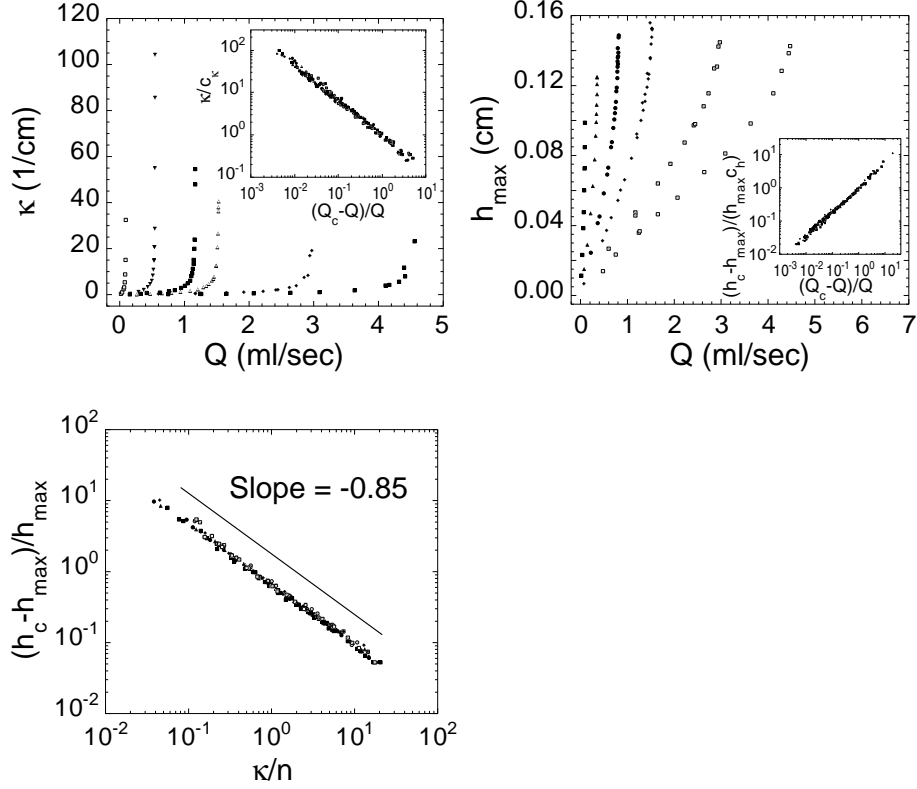


Figure 3: Scaling for the mean hump tip curvature, κ , and height h_{max} . 3a plots κ vs. Q for six tube heights. Each curve displays diverging behavior with increasing Q . For each tube height we choose a critical flow rate Q_c as a fitting parameter and show (3a inset) that as Q approaches Q_c the curvatures increase as power laws. The prefactors to the curvature power laws, $c_\kappa(S)$, are scaled out in the inset. Figure 3b plots h_{max} vs. Q for six tube heights. For each S we choose a critical hump height h_c as a fitting parameter. As Q approaches Q_c (taken from 3a inset), the hump heights approach the critical heights as power-laws. The prefactors, $c_h(S)$, to the power laws in the inset are scaled out. Figure 3c plots $(h_c - h_{max})/h_{max}$ vs. κ/n for the entire data set corresponding to fifteen different straw heights. The prefactor n roughly decreases as $\exp^{-2.5S}$. The line corresponds to a power-law with an exponent of -0.85.

$\exp^{-2.5S}$. Here, we correlate this decrease with the observation that the profiles become shallower at larger S . The points of deviation for the $S = 0.255$ cm and 0.381 cm profiles mark the transition from the similarity regime to the matching regime beyond which the profiles become asymptotically flat. At large enough radii all of the scaled profiles display these deviations.

We have shown that in the $Q > 0.1$, ml/sec regime, a similarity analysis can be used to describe the flows near the selective-withdrawal transition [16]. We have observed power-law scaling of the hump height and curvature (Fig. 3) and used these scaling relations to collapse the hump profiles at different flow rates and tube heights onto a single universal curve (Fig. 4). However, the origin of the saturation of κ at large Q remains an important unexplained problem. Further insight into this cutoff behavior may be gained by comparing with an analogous two-dimensional (2-D) problem which roughly corresponds to replacing the tube with a line sink. Jeong and Moffatt [17] showed that in an idealized case where the bottom fluid is inviscid while the top fluid is very viscous, the 2-D hump interface forms a 2-D cusp singularity above sufficiently high withdrawal rates. Recently, Eggers [18] showed that the solution changes when the lower fluid has a finite viscosity; the system no longer manifests a singularity [19]. Instead, the approach to the singularity is cut off and the system undergoes a transition to a different steady state. In this new state, a sheet of the lower fluid is entrained along with the upper fluid into the line sink. However, the finite lower fluid viscosity prevents the hump profiles from scaling onto a similarity solution.

Here, we have shown that for the three-dimensional selective withdrawal system even when both fluids are viscous ($\eta > 1$ St for both fluids) the effects of a singularity manifest themselves in the scaling of the hump profiles. Furthermore, preliminary experiments show that a reduction of the lower fluid viscosity to 0.01 St has little effect in determining the final curvature of the hump tip or equivalently, how close the system is to forming a cusp. This suggests that for our 3-D problem, either the effects of the lower fluid viscosity enter as a higher-order perturbation to the profile shapes, or a different mechanism underlies the avoidance of the cusp formation. If the latter scenario is correct, it may be possible for the system to manifest the singularity at a finite lower fluid viscosity. In either case, determining which variables affect how close the system approaches the singularity would allow for control of the maximum hump curvature and minimum spout diameter. This control could then be used to advance technologies such as coating microparticles [20], creating mono-dispersed micro-spheres [21], and emulsification through tip streaming [18, 22] which take advantage of the selective withdrawal geometry.

We are grateful to W. W. Zhang, S. Venkataramani, J. Eggers, H. A. Stone, T. J. Singler, J. N. Israelachvili, C. C. Park, S. Chaieb, S. N. Coppersmith, T. A. Witten, L. P. Kadanoff, R. Rosner, P. Constantin, R. Scott, T. Dupont H. Diamant, and V. C. Prabhakar for sharing their insights. This research is supported by the University of Chicago (MRSEC) NSF DMR-0089081 grant

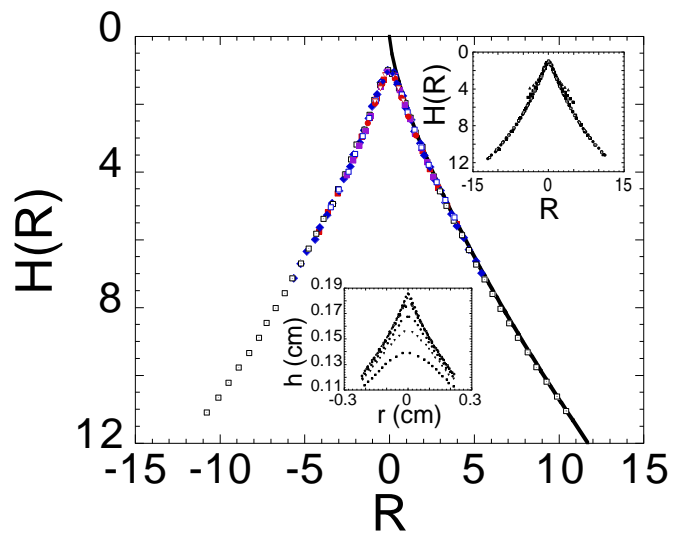


Figure 4: The scaled hump profiles. The lower inset shows eight profiles taken from the $S = 0.830$ data set. The main figure shows the same profiles after scaling. The solid line corresponds to a power law of the form $R^{0.72}$. In the upper inset we compare the universal curves for the $S = 0.830$ cm, 0.613 cm, 0.508 cm, 0.381 cm, 0.255 cm data sets.

References

- [1] in *Singularities in Fluids, Plasmas, and Optics*, edited by R. E. Caflisch & G. C. Papanicolaou (Kluwer, Norwell, MA, 1993).
- [2] A. L. Bertozzi, M. P. Brenner, T. F. Dupont, & L. P. Kadanoff, in *Trends and Perspectives in Applied Mathematics*, edited by L. Sirovich (Springer, New York, 1994).
- [3] R. E. Goldstein, A. I. Pesci, & M. J. Shelley, *Phys. Rev. Lett.* **70**, 3043 (1993).
- [4] M. Pugh & M. J. Shelley, *Comm. Pure App. Math.* **51**, 733 (1998).
- [5] G. I. Barenblatt, *Scaling, self-similarity and intermediate asymptotics* (Cambridge University Press, Cambridge, UK, 1996).
- [6] J. R. Lister & H. A. Stone, *Phys. Fluids* **10**, 2758 (1998).
- [7] D. Bensimon *et al.*, *Rev. Mod. Phys.* **58**, 1986 (1986).
- [8] S. R. Nagel & L. Oddershede, *Phys. Rev. Lett.* **85**, 1234 (2000).
- [9] B. W. Zeff, B. Kleber, J. Fineberg, & D. P. Lathrop, *Nature* **403**, 401 (2000).
- [10] I. Cohen, to be published.
- [11] A. W. Neumann & J. K. Spelt, *Applied Surface Thermodynamics* (Marcel Dekker, New York, 1995).
- [12] F. K. Hansen & G. Rodsrud, *J. Colloid Interface Sci.* **141**, 1 (1991).
- [13] J. R. Lister, *J. Fluid Mech.* **198**, 231 (1989).
- [14] For systems with a different upper fluid viscosity, we find that the power-law dependence changes. There is a vast literature which focuses on explaining the Su vs. Q dependence (e.g. [13]). We therefore defer the detailed discussion of how currently available scaling predictions compare with the data to [10].
- [15] Note that the transition from spout to hump is also discontinuous indicating that there is a curvature cut-off for the spout states as well. Since surfactants are continuously being removed from the interface when the system is in the spout state, the presence of surfactants in our system is not enough to account for the discontinuous nature of the transition or equivalently the values of the curvature cut-offs. More generally, we find that surfactant effects do not significantly influence the results presented. A more detailed discussion is presented in [10].

- [16] While scaling has been hypothesized for an analogous 3-D system [A. Acrivos and T. S. Lo, *J. Fluid Mech.* **86**, 641, (1978)] it was never shown experimentally.
- [17] J. T. Jeong & H. K. Moffatt, *J. Fluid Mech.* **241**, 1 (1992).
- [18] J. Eggers, *Phys. Rev. Lett.* **86**, 4290 (2001).
- [19] J. Eggers, *Rev. Mod. Phys.* **69**, 865 (1997).
- [20] I. Cohen *et al.*, *Science* **292**, (2001).
- [21] A. M. Ganan-Calvo, *Phys. Rev. Lett.* **80**, 285 (1998).
- [22] J. D. Sherwood, *J. Fluid Mech.* **144**, 281 (1984).